Physics of the Earth and Planetary Interiors, 34 (1984) 24–45
Elsevier Science Publishers B.V., Amsterdam – Printed in The Netherlands

An earthquake doublet in Ometepec, Guerrero, Mexico

Luciana Astiz and Hiroo Kanamori

Seismological Laboratory, California Institute of Technology, Pasadena, CA 91125 (U.S.A.)

(Received August 12, 1983; accepted October 10, 1983)

Astiz, L. and Kanamori, H., 1984. An earthquake doublet in Ometepec, Guerrero, Mexico. Phys. Earth Planet. Inter., 34: 24–45.

On June 7, 1982 an earthquake doublet occurred in a gap near Ometepec, Guerrero, Mexico which had been given a high seismic potential. The two earthquakes (first event: $M_s = 6.9$, $m_b = 6.0$, 16.3°N, 98.4°W, $d = 25$ km; second event $M_s = 7.0$, $m_b = 6.3$, 16.4°N, 98.5°W, $d = 8$ km) of the doublet occurred within five hours of each other.

We determine the source parameters of these events by inverting surface-wave data at a period of 256 s. The results are for the first event, strike = 116°, dip = 77°, slip = 88° and seismic moment of 2.8×10^{26} dyne · cm, and for the second event strike = 116°, dip = 78°, slip = 89° and seismic moment of 2.8×10^{26} dyne · cm. Modeling of long-period P waves suggests that the first event has a depth of 20 km and is represented by a single trapezoidal source time function, with an effective duration of 6 s. The second event is best modeled by two sources at depths of 15 and 10 km. The combined effective source duration time for the two sources is about 10 s. The ratio of the seismic moment, obtained from body waves to that from surface waves, is ~ 0.5 for the first event and 1 for the second. Adding the seismic moment of the two events and considering the first week aftershock area, 3200 km^2, the stress drop is ~ 4 bars. These results suggest that the first event, that involved a deeper asperity, caused an incremental stress change large enough to trigger the second event. If the two events of the doublet broke distinct areas of the subduction zone, the coseismic slip is 0.58 m, and accounts for about 25% of the total plate motion between the Cocos Plate and the North America Plate, accumulated since the last large earthquake in the region.

Other doublets similar to the Ometepec doublet have occurred along the Middle America Trench during the past 70 years. A regional distribution of comparable-size asperities may be responsible for this relatively frequent occurrence of doublets and for the simplicity of earthquakes in the region. The high convergence rate, which produces rapid strain accumulation and short recurrence intervals for large earthquakes, and the smooth sea-floor subducted along the middle America Trench, may contribute to the homogeneous distribution of comparable size asperities.

We found a relation, $\log T \approx 1/3 \log M_0$ (T is the average recurrence time and M_0 is the average seismic moment) for large earthquakes along the subduction zone in the Guerrero–Oaxaca region, where the convergence rate and the properties of the subducted plate are considered relatively uniform. A simple asperity model predicts this relation.

1. Introduction

One June 7, 1982, an earthquake doublet occurred in Ometepec, Guerrero, Mexico. The two earthquakes of the doublet occurred within five hours of each other. The U.S.G.S. location of the first event ($M_s = 6.9$, $m_b = 6.0$) is 16.607°N, 98.149°W, 40.5 km depth and the origin time is 06h 52 min 37.37; that of the second event ($M_s = 7.0$, $m_b = 6.3$) is 16.558°N, 98.358°W, 33.8 km depth, and the origin time is 10 h 59 min 40.16 s. The epicenters given by a local network are 16.348°N, 98.368°W, 25 km depth (origin time 06 h 52 min 33.7 s) for the first event, 16.399°N, 98.538°W, 8 km depth (origin time 10 h 59 min 40.1 s) for the second event. The locally determined epicenters are shallower than, and to the southwest of, the U.S.G.S. locations (Fig. 2b), as is typically found for events along the Mexican subduction zone (e.g., Havskov et al., 1983). Hereafter, these two events are referred to as 1982 [1] and 1982 [2], respectively.

0031-9201/84/$03.00

The Ometepec doublet events occurred in a gap which had been given a high seismic potential (Singh et al., 1981). A study of these events is therefore important for a better understanding of the failure mechanism of seismic gaps. We determine the rupture process of the Ometepec doublet by detailed analysis of surface and body waves. We find that the Ometepec doublet has many features in common with similar doublets observed in other regions. The Ometepec doublet events are somewhat smaller than the large earthquakes characteristic of the Middle America subduction zone, and the average repeat time in the Ometepec region is slightly shorter than in the adjacent segments of the Guerrero–Oaxaca regions. We will show that these features can be explained by a heterogeneous strength distribution in the fault zone along the Middle America Trench.

Owing to the high seismic activity and the relatively short (30–50 years) recurrence times of large events along the Middle America Trench, many detailed studies have recently been conducted on individual earthquakes (e.g., Ohtake et al., 1977; Yamamoto, 1978; Reyes et al., 1979; Espindola et al., 1981; Stewart et al., 1981; Chael and Stewart, 1982; Lefevre and McNally, 1982; Valdés et al., 1982; Wang et al., 1982; Tajima and McNally, 1983; Havskov et al., 1983) as well as on the regional seismicity (e.g., Kelleher et al., 1973; McNally and Minster, 1981; Singh et al., 1981; Lefevre and McNally, 1982; Singh et al., 1982b). These studies suggest that large earthquakes occur repeatedly at places with increased mechanical strength, which are often called asperities in the

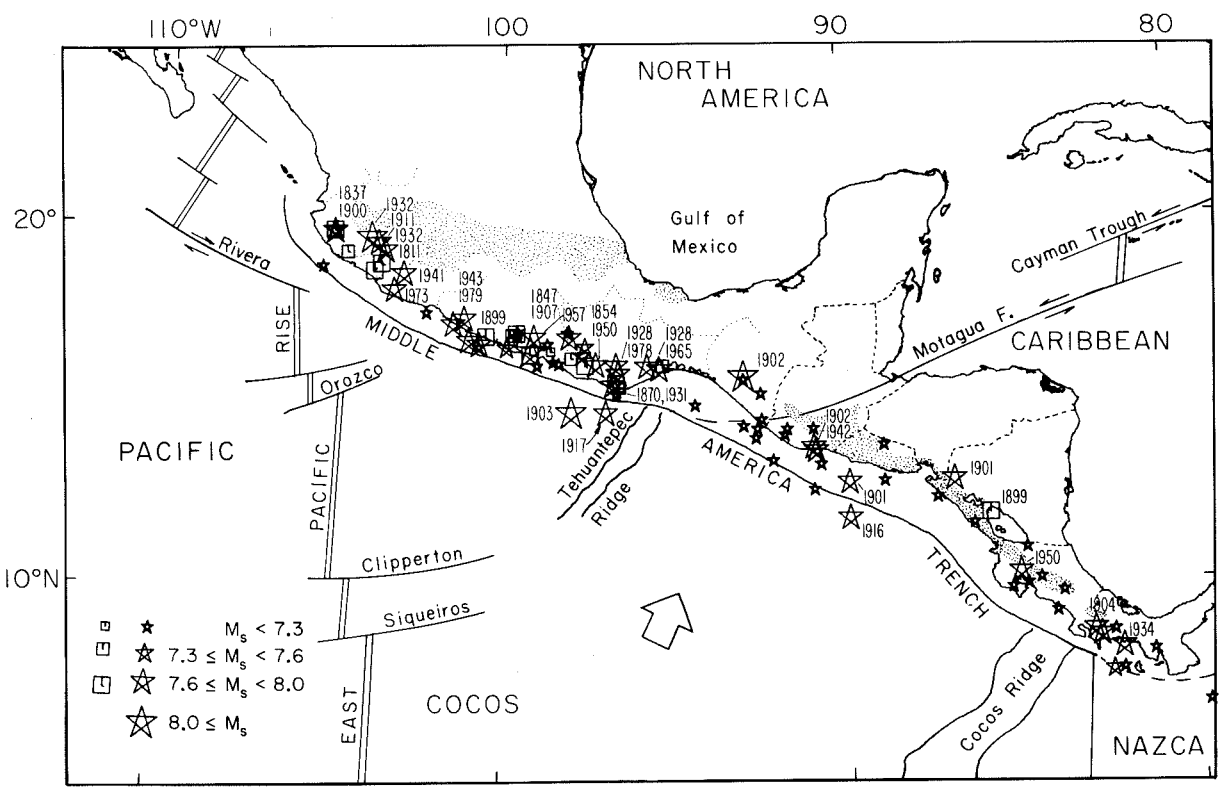

Fig. 1. Main tectonic features of Middle America, simplified after Mammerickx et al. (1975). The arrow indicates the mean direction of convergence between the Cocos and North America and Caribbean Plates. Shaded areas delineate the Quaternary Volcano alignments in Mexico and Central America. Shallow large earthquakes which ($M_s \geq 7$) occurred along the Middle America Trench are shown. Squares correspond to last century events and stars to those which occurred during this century. The year of occurrence is indicated for events with $M_s > 7.5$.

recent literature. Singh et al. (1982b) infer a distribution of relatively homogeneous size asperities along the Mexican subduction zone from the magnitude-frequency relations for large earthquakes. Our results, together with those of previous investigators, suggest that the fault zone heterogeneity, characterized by the asperity distribution, plays a key role in controlling the recurrence time and the triggering mechanism of large earthquakes.

1.1. Tectonic setting

The Middle America Trench is a continuous topographic feature that extends mostly parallel to the southwest coast of Mexico and Central America for about 3000 km (Fisher, 1961). Along the trench the Cocos Plate is subducted beneath the North America and Caribbean Plates (Molnar and Sykes, 1969; Dean and Drake, 1978). The Cocos Plate dips gently (10–20°) beneath the North America Plate (Chael and Stewart, 1982) and more steeply below the Caribbean Plate (Molnar and Sykes, 1969). The triple junction of these plates is not well established, but it is probably located in the Tehuantepec Gulf region where the projection of the Cayman Trough–Motagua transform fault system, which is the boundary of the Caribbean and North American Plates, intersects the Middle America Trench (Plafker, 1976). Seaward from the trench, relative structural homogeneity of the seafloor is observed, interrupted only by the Rivera and Orozco fracture zones and the Tehuantepec and Cocos Ridges (Fig. 1). However, the continental margin shows a duality. Northwestward of the Tehuantepec Ridge the continental margin is narrow, with numerous submarine canyons, and trench turbidities are presently being accreted. Southeast of the ridge, the continental margin is wide with a well developed fore-arc basin and no observed accretion (Shipley et al., 1980; Aubouin et al., 1981). Gravity anomalies offshore of southern Mexico and northwestern Guatemala support the above observations (Couch and Woodcock, 1981). The shaded area in Fig. 1 shows the line of active volcanoes that, in the Central America region,

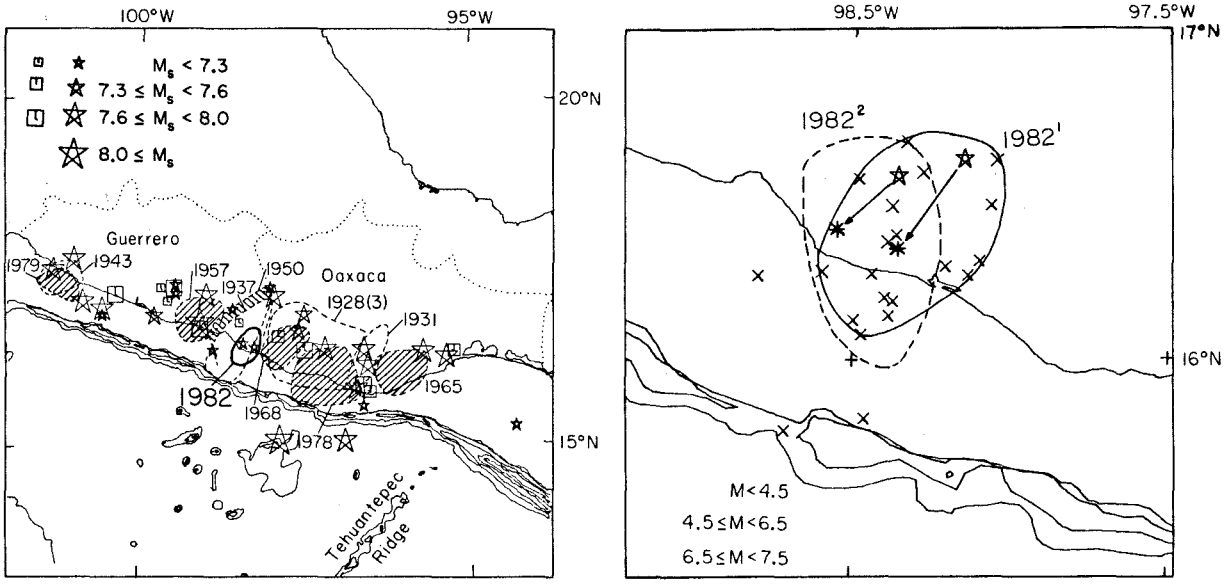

Fig. 2. (a) Aftershock areas of large shallow interplate earthquakes along the Mexican subduction zone, between the Orozco fracture zone and the Tehuantepec Ridge (after Kelleher et al., 1973; Singh et al., 1980b; Valdés et al., 1982). Shaded areas correspond to more recent events. The Ometepec doublet aftershock area defined by the events with $m_b \geq 3.6$ (from P.D.E.) which occurred during the first week of activity is shown by the heavy solid curve. (b) The heavy curve indicates the Ometepec doublet aftershock area shown in Fig. 2a. The dashed curve indicates the first week aftershock area and the solid stars the Ometepec doublet epicenters determined by Nava (1983) using a local network. Only events located within 20 km of each other are included in the aftershock areas.

forms a prominent chain parallel to the trench and 150 km to the east (Stoiber and Carr, 1973). In contrast, in the Mexico segment, the Mexican Volcanic Belt is oblique to the trench and is located 200–300 km away from it (Mooser, 1972; Demaint, 1978).

During this century numerous large shallow earthquakes ($M \geq 7$) have occurred along the Middle America Trench in discrete segments 100–200 km long with recurrence intervals in each segment of 30–50 years (Kelleher et al., 1973; McNally and Minster, 1981; Singh et al., 1981). However, in the Tehuantepec region, no large shallow earthquake has occurred for the last 180 years. This gap is considered to be either aseismic, or seismic with anomalously large recurrence times (McCann et al., 1979; Singh et al., 1980a). Epicenters of large shallow earthquakes ($M \geq 7$) along the Middle America Trench are shown in Fig. 1. Squares indicate last-century's events and stars this century's events. Dates are shown for the events with $M_s > 7.5$.

A detailed study of source parameters of six large shallow (15–20 km) earthquakes from 1965–1979 along the Middle America Trench (Chael and Stewart, 1982) and of the 1981 Playa Azul, Michoacán, earthquake (Lefevre and McNally, 1982) has shown remarkably simple fault processes for these events at long periods (10 s or longer), with stress drops from 1 to 10 bars and seismic moments from 1 to 3.2×10^{27} dyne · cm (see Table VII). The focal mechanisms of these events indicate thrusting, consistent with the subduction of the Cocos Plate to the northeast (Minster and Jordan, 1978).

Singh et al. (1981) identified a seismic gap on the Ometepec region based on aftershock areas and recurrence intervals of large earthquakes. Figure 2a shows the aftershock area of previous earthquakes in the Guerrero–Oaxaca region with dashed lines (after Kelleher et al., 1973; Singh et al., 1980b and Valdés et al., 1982). Shaded areas correspond to more recent events. The location of the 1982 Ometepec doublet and the aftershock distribution of events $m_b \geq 3.6$, during the first week of activity, as reported by the Preliminary Determination of Epicenters of the U.S. Geological Survey (P.D.E.), is shown by the heavy solid curve (Fig. 2). The aftershock area is about 3200 km^2 (78×41 km). The dashed curve indicates the first week aftershock area and the solid stars are the Ometepec doublet epicenters given by Nava (1983) (Fig. 2b). The locally determined aftershock area is about 3300 km^2 (82×40 km). Only events located within 20 km of each other are included in the aftershock areas. Large interplate earthquakes in the Ometepec region occurred on December 2, 1890 ($M_s = 7.3$), December 23, 1937 ($M_s = 7.5$) and December 14, 1950 ($M_s = 7.3$) giving an average recurrence interval of 30 years. Miyamura (1976) reports a $M_s = 7.0$ event in this region on December 28, 1951; however, Figueroa (1970) gives this event $M_s = 6.5$. In any case, the 1950 earthquake and the 1951 event can be considered as part of the same seismic sequence. Notice that the 1957 Acapulco ($M_s = 7.5$) and the 1968 Oaxaca ($M_s = 7.4$) earthquakes did not break the Ometepec segment.

Seismic reflection and geologic surveys of the region during 1977 and 1978 by Shipley et al. (1980) reveal significant variations in structure over short distances, suggesting that the extent of aftershock activity may be controlled by structural

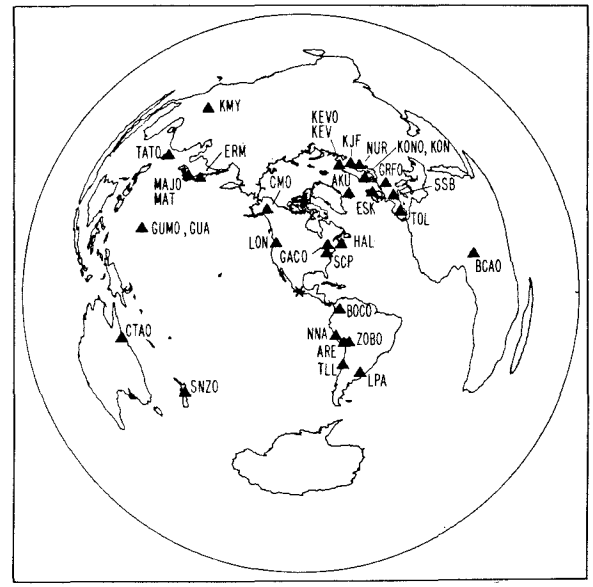

Fig. 3. Azimuthal equidistant world map centered at the Ometepec, Mexico, doublet epicentral area (16.5°N, 98.2°W). The triangles indicate the location of WWSSN, GDSN and IDA stations used in this study.

TABLE I

Stations used in the body- and surface-wave analysis

Station	Location	Type	Δ (deg)	Az (deg)	Phases used					
					1982 [1]			1982 [2]		
KEVO	Kevo, Finland	DWWSS	86.0	16.5	P			P		
KEV	Kevo, Finland	WWSS	86.0	16.5	P			P		
KJF	Kajaam, Finland		89.6	20.7	P			P		
NUR	Nurmijarvi, Finland	WWSS	90.9	24.4	P			P		
AKU	Akureyri, Iceland	WWSS	71.2	25.5				P		
GACO	Glen Almond, Canada	SRO	34.9	28.4	P	R2, R3	G3	P		G3
SSB	Saint-Sauveur, France	IDA	87.4	43.4		R1, R2			R2	
KONO	Kongsberg, Norway	ASRO	84.8	28.9	P	R1, R2	G1, G2	P	R2, R3	G1, G2
KON	Kongsberg, Norway	WWSS	84.8	28.9	P			P		
SCP	State College, PA, U.S.A.	DWWSS	30.2	31.9	P			P		
ESK	Eskdalemuir, Scotland	WWSS	79.6	35.3	P			P		
GRFO	Grafenberg, Germany	SRO	89.8	37.6	P	R2, R3	G3	P	R2, R3	G2, G3
HAL	Halifax, N.S., Canada	IDA	40.3	38.7		R2, R3			R2	
TOL	Toledo, Spain	WWSS	82.9	50.5	P			P		
BCAO	Bangui, Central Afr. Rep.	SRO	114.3	77.1			G1			G1
BOCO	Bogota, Colombia	SRO	26.5	113.5		R2, R3	G2		R2, R3	G2, G3
ZOBO	Zongo Valley, Bolivia	ASRO	44.1	135.8	P		G2	P		G2
ARE	Arequipa, Peru	WWSS	42.1	139.5	P			P		
NNA	Nana, Peru	WWSS, IDA	35.4	143.4	P			P		
LPA	La Plata, Argentina	WWSS	63.9	143.4	P			P		
TLL	Tololo, Chile		53.3	150.0	P					
SNZO	South Karori, New Zealand	SRO	98.3	229.6	P	R2	G1, G2	P	R1, R2	G1, G2
CTAO	Charters Towers, Australia	ASRO	118.8	255.9	P	R1, R2	G2, G3		R1, R2	G1, G2
GUA	Guam, Mariana Island	IDA	110.7	291.8		R2			R2	
GUMO	Guam, Mariana Island	SRO	110.7	291.8		R1, R2	G2, G3	P	R1, R2	G2, G3
TATO	Taipei, Taiwan	SRO	123.3	315.8	P	R1, R2		P	R1, R2	G3
MAJO	Matsushiro, Japan	ASRO	105.0	315.9	P	R2	G1, G2	P	R2, R3	G2, G3
MAT	Matsushiro, Japan	WWSS	105.0	315.9	P			P		
ERM	Erimo, Japan	IDA	98.8	318.5		R2			R2	
LON	Longmire, WA, U.S.A.	DWWSS	36.0	332.4	P			P		
KMY	Kunming, P.R.C.	IDA	133.8	333.1		R1, R2			R1, R2	
CMO	College, AK, U.S.A.	IDA	58.6	337.6		R2, R3			R2, R3	

features. The Ometepec Canyon is right-laterally displaced seaward of the trench, suggesting oblique subduction along the Middle America Trench. During this survey, sediments on the Ometepec Canyon appeared undisturbed along the trench, indicating that this segment had not been broken recently.

2. Data analysis

Long-period recordings of the 1982 Ometepec, Mexico, doublet by the Worldwide Standardized Seismograph Network (WWSSN), the Global Digital Seismograph Network (GDSN) and the International Deployment of Accelerograph (IDA) are used in the present study. Station distribution around the doublet epicentral area (16.5°N, 98.2°W) is shown in Fig. 3 and the stations used for body- and surface-wave analysis for both events are listed in Table I. Surface-wave analysis for large events gives first order estimates of source orientation and seismic moment at long periods (180–350 s) (e.g., Kanamori and Given; 1981, 1982; Lay et al., 1982). Body-wave modeling can determine the depth, the detailed source time history of the event, and the seismic moment at shorter periods (e.g., Kanamori and Stewart, 1976; Eissler and Kanamori, 1982).

2.1. Surface-wave analysis

We use the inversion method described by Kanamori and Given (1981) for long-period surface waves to determine the source parameters from Rayleigh and Love waves recorded on the GDSN and IDA network. We filter all phases R1–R3 and G1–G3 between 60 and 1500 s, and discard the R1 and G1 waves contaminated by nonlinear transients. We first compute the amplitude and phase spectra of both Rayleigh and Love waves at a period of 256 s. Redundant pairs (e.g., R1 and R3) give consistent results in most cases, ensuring good quality data.

We then invert the spectral data to obtain the 5 moment tensor elements M_{xx}, M_{yy}, M_{xy}, M_{zz} and M_{zy} assuming that the isotropic component is zero. However, as discussed by Kanamori and Given (1981), two of the five elements, M_{zx} and M_{zy} become indeterminate for shallow ($d \leq 30$ km) events. In order to overcome this difficulty we invert the data using three different sets of constraints.

First, following Kanamori and Given (1981), we set $M_{xz} = M_{yz} = 0$, which is equivalent to restricting the solution either to a 45° dip-slip or to a vertical strike-slip fault. Despite this restriction, the solutions obtained with these constraints provide useful gross estimates of fault geometry and

TABLE II

Constrained solutions of moment tensor inversion

Data	1982 [1]		1982 [2]	
Inversion constraints	$T = 256$ s, $d = 33$ km, $\tau = 12$ s		$T = 256$ s, $d = 16$ km, $\tau = 16$ s	
	$M_{xz} = M_{yz} = 0$	$\alpha = -0.42$ $\beta = +0.96$ $M_r = M_{xx} + M_{yy}$	$M_{xz} = M_{yz} = 0$	$\alpha = +0.16$ $\beta = -1.96$ $M_r = M_{xx} + M_{yy}$
M_{xy} [a]	0.041 ± 0.007	0.041 ± 0.007	0.035 ± 0.008	0.036 ± 0.008
$M_{xx} - M_{yy}$	0.046 ± 0.012	0.046 ± 0.012	0.044 ± 0.013	0.049 ± 0.013
$M_{xx} + M_{yy}$	-0.126 ± 0.010	-0.119 ± 0.011	-0.113 ± 0.011	-0.114 ± 0.014
M_{yz}	0.0	0.051 ± 0.0	0.0	0.008 ± 0.0
M_{xz}	0.0	-0.115 ± 0.0	0.0	-0.096 ± 0.0
M_0 (10^{26} dyne·cm)	1.26	1.76	1.13	1.53
Dip (δ)	45.0°	21.2°, 68.9°	45.0°	25.8°, 66.1°
Strike (φ)	300.3°	303.6°, 115.5°	298.9°	307.2°, 103.5°
Slip (λ)	90.0°	97.5°, 87.1°	90.0°	111.5°, 79.9°
% minor D–C	7.86%	12.79%	7.62%	7.83%

[a] Unit of the moment tensor elements in 10^{27} dyne·cm.

TABLE III

Fault constrained solutions

Data	1982 [1]		1982 [2]	
	$T = 256$ s, $d = 33$ km, $\tau = 12$ s		$T = 256$ s, $d = 16$ km, $\tau = 16$ s	
	Ampl. Phase	Amplitude	Ampl. Phase	Amplitude
M_0 (10^{26} dyne·cm)	2.35	2.82	2.42	2.75
Dip (δ)	77.0°, 13.0°	77.0°, 13.0°	78.0°, 12.0°	78.0°, 12.0°
Strike (φ)	116.0°, 296.7°	116.0°, 277.2°	116.0°, 302.4°	116.0°, 274°
Slip (λ)	88.3°, 97.0°	94.3°, 69.5°	88.7°, 96.0°	94.9°, 68.0°
R.M.S.	0.47	0.05	0.53	0.12
M_w	6.85	6.90	6.86	6.89

seismic moments. In the following, these solutions are called "constrained moment tensor solutions".

An alternative method is to use the P-wave first-motion data to determine the source parameters that are not resolvable by surface-wave data. Implicit in this method is the assumption that the same fault geometry is responsible for both P- and surface-wave radiations. It is often possible to determine one of the nodal planes by P-wave first motion data. In such a case, we constrain the parameters (dip angle and strike) of this nodal plane and invert the surface-wave data to determine the other nodal plane and the seismic moment. We call this type of solution "fault constrained solution".

When the P-wave data do not completely con-

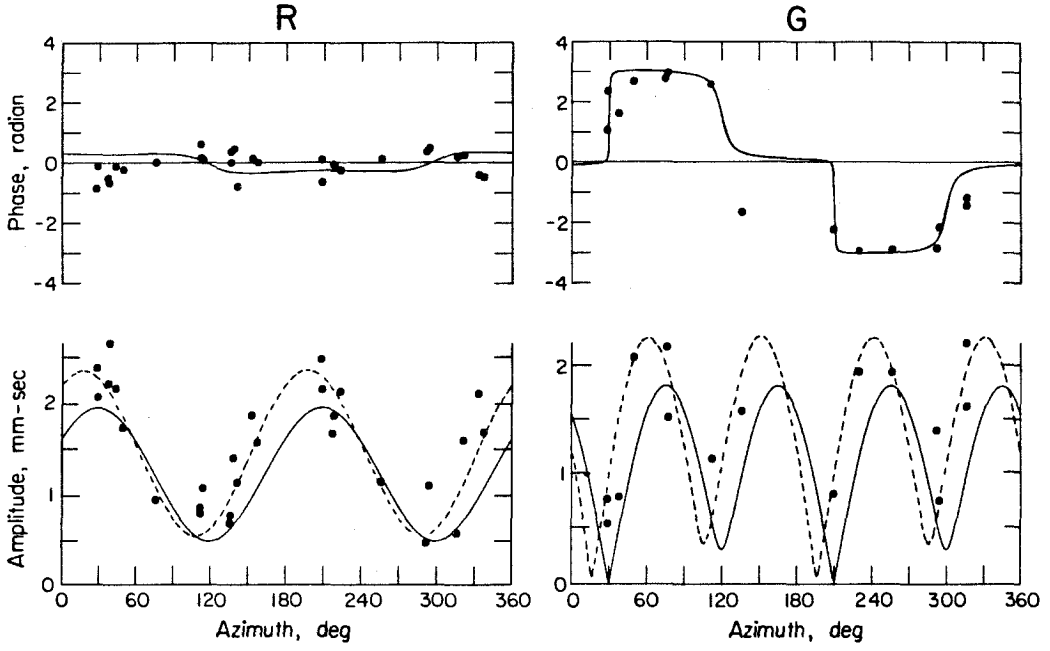

Fig. 4. Phase and amplitude spectra of Rayleigh and Love waves at 256 s period of the 1982 [1] Ometepec earthquake (June 7, 1982 06 h 52 min). The phase spectra have been corrected for source finiteness using $\tau = 12$ s. The solutions are listed in Table III. The solid curves are for the solution obtained by inversion of the amplitude and phase data and the dotted curves are for the solution obtained from the amplitude data alone.

strain one of the nodal planes, we use a third method described in detail by Kanamori (1983). In this method, we constrain M_{zx} and M_{zy} with respect to the moment tensor element with the largest absolute value, M_r, (i.e., $M_r = M_{xy}$, $M_{zz} + M_{yy}$ or $M_{xx} - M_{yy}$) such that the ratios $\alpha = M_{zy}/M_r$ and $\beta = M_{zx}/M_r$ are consistent with P-wave first-motion data. Hereafter, we call this solution "P-wave constrained solution".

The fault finiteness and the finite rise time of the source dislocation function introduce a source phase delay. For events with fault lengths less than 100 km this effect can be included by use of a source process time τ, which can be empirically estimated from the earthquake magnitude (Kanamori and Given, 1981; Nakanishi and Kanamori, 1982). The source process times τ obtained from table III of Kanamori and Given (1981) for the first and second events of the Ometepec doublet, are 12 and 16 s, respectively. For the inversion, we use a point source at a depth of 33 km for the first event and 16 km for the second event. Although the source depth cannot be resolved in detail by long-period surface waves, they do indicate that both events are shallow. Results of the inversion, using the three methods described above, are listed in Tables II and III. Table II presents a comparison of the constrained solution and the P-wave constrained solution, for which the two fault planes are listed. Table III lists the source parameters determined by inversion of surface-wave data with the steeply-dipping nodal plane (dip and strike) constrained by the P-wave first-motion data (Figs. 6 and 8). In this inversion, the depth and source process time τ, are the same as those used in the moment tensor inversions.

The solutions obtained by all three methods have about the same strike and slip angle which are consistent with subduction of the Cocos Plate beneath Middle America. The similarity of these solutions indicates that the surface waves and the body waves are radiated from sources with similar geometry for these two earthquakes. Since the steeply-dipping nodal plane is very tightly constrained by the body-wave data, we prefer the fault constrained solutions given in Table III. Ta-

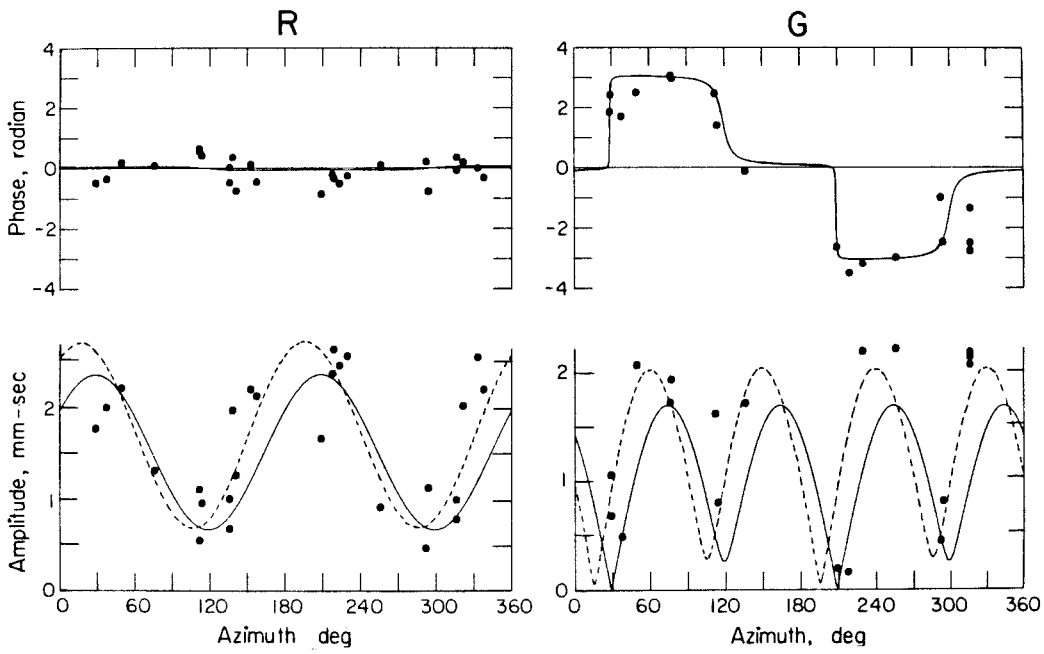

Fig. 5. Phase and amplitude spectra of Rayleigh and Love waves at 256 s period of the 1982 [2] Ometepec earthquake (June 7, 1982 10 h 59 min). The phase spectra have been corrected for source finiteness using $\tau = 16$ s. The solutions are listed in Table III. The solid curves are for the solution obtained by inversion of the amplitude and phase data and the dotted curves are for the solution obtained from the amplitude data alone.

ble III includes the results of inversion of the amplitude data alone, which have slightly higher moments than those obtained by inversion of both amplitude and phase data. This trend is caused by a slight mismatch of the phase data due to the lateral heterogeneity of the Earth, and is commonly seen in this type of inversion (see Nakanishi and Kanamori, 1982; Lay et al., 1982). The comparison of the data with the calculated amplitude and phase spectra is shown in Figs. 4 and 5. The continuous line is the result of the amplitude and phase data inversion and the dashed line is the result of the amplitude inversion. In view of the good fit to the amplitude data, we use the results obtained by inversion of amplitude data in the following discussion.

In 1982, as part of the U.S.G.S. monthly listing of epicenters, a preliminary moment tensor solution by Dziewonski et al. (1981) is given for all events $M > 5.5$. The fault parameters they obtain for the Ometepec doublet are: $M_0 = 2.9 \times 10^{26}$ dyne · cm, $\phi_1 = 268°$, $\delta_1 = 10°$, $\lambda_1 = 48°$, $\phi_2 = 130°$, $\delta_2 = 83°$ and $\lambda_2 = 9°$ for the first event and $M_0 = 2.7 \times 10^{26}$ dyne · cm, $\phi_1 = 286°$, $\delta_1 = 12°$, $\lambda_1 = 76°$, $\phi_2 = 121°$, $\delta_2 = 79°$, and $\lambda_2 = 93°$ for the second event. Our solutions agree reasonably well with these results.

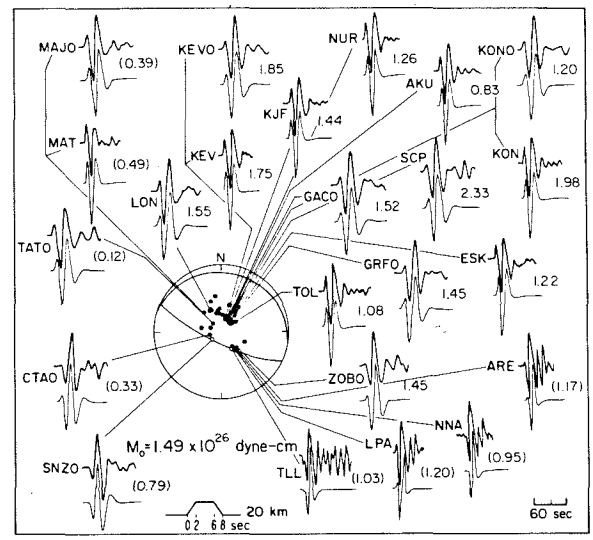

Fig. 6. Observed (upper) and synthetic (lower) P-waves seismograms of the 1982 [1] Ometepec event (June 7, 1982 06 h 52 min). The synthetics correspond to the focal mechanism, depth and source time function shown. The seismic moment at each station is given in 10^{26} dyne·cm. The average, $M_0 = 1.49 \times 10^{26}$ dyne·cm, is computed with the values of non-nodal stations within a distance range from 30–90°. Values in parentheses are excluded.

2.2. *Body-wave modeling*

P-waves recorded by long-period seismographs of 22 WWSSN and GDSN stations (Table I) are modeled for each event of the 1982 Ometepec doublet. Some of the P-waves modeled were recorded by stations of both seismic networks at the same location.

We compute synthetic seismograms using the method described in detail by Langston and Helmberger (1975) and Kanamori and Stewart (1976). First, the response of a homogeneous half space to a properly oriented point double-couple source with a trapezoidal time function defined by three time constants (t_1, t_2, t_3) (see Kanamori and Stewart, 1976, fig. 9) is computed. The direct P and surface reflected phases pP and sP are included. Then the attenuation operator and the instrument response are convolved, to obtain the synthetic seismogram. Using the synthetic seismograms thus computed, we determine the source orientation, depth and the dimensions of the trapezoidal time function. Near-nodal stations are important to determine the source orientation. Although there is some trade-off between the source depth and time function in fitting the observed seismogram at a particular station, use of many stations distributed over a large azimuthal range reduces this trade-off significantly.

In order to compare the fault parameters of the Ometepec doublet directly with those of other large earthquakes along the Middle America Trench, we use the same velocity model as that used by Chael and Stewart (1982): $v_p = 6.1$ km s^{-1}, $v_s = 3.5$ km s^{-1} and $\rho = 2.6$ g cm^{-3}. The Ometepec doublet has simple waveforms, like other large shallow earthquakes ($M_s > 7$) along the Middle America Trench (see Fig. 9).

Figure 6 shows the observed and synthetic P-waves recorded at 22 WWSSN and GDSN stations for the 1982 [1] Ometepec event (June 7, 1982,

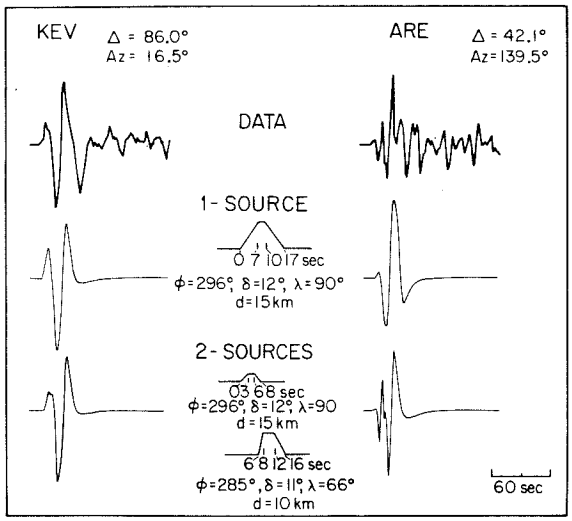

Fig. 7. Comparison of 1-Source and 2-Source models for KEV and ARE. Notice that the 1-Source model can explain the overall waveform observed at KEV, but it fails to match that of ARE (near-nodal). The 2-Source model can fit the wave-forms at both stations.

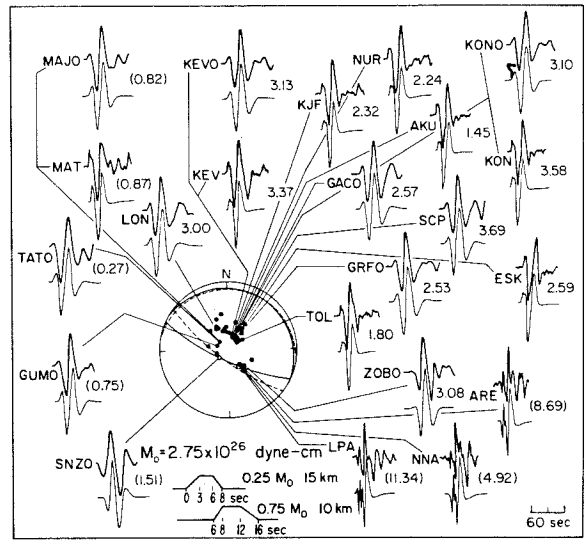

Fig. 8. Observed (upper) and synthetic (lower) P-waves of the 1982 ^{2} Ometepec event (June 7, 1982 10 h 59 min). the focal mechanism in the middle indicates the geometry of the first source (continuous line) and the second source (dashed line) used for the P-wave modeling. The source time function, depth and the seismic moment ratio for each source are shown. The seismic moment at each station is given in 10^{26} dyne·cm. The values at non-nodal stations within a distance range from 30 to 90° are used to calculate the average seismic moment, $M_0 = 2.75 \times 10^{26}$ dyne·cm. Values of stations in parentheses are not included.

06 h 52 min). The source orientation can be resolved within a few degrees, since near-nodal records are available. The source time function obtained is (2, 6, 8) for a point source depth of 20 km. The depth and rupture time can be resolved within ± 3 km and ± 1 s for a given velocity model. The seismic moment at each station is given in Fig. 6 and the average moment at non-nodal stations within a distance range from 30 to 90° is $M_0 = 1.5 \pm 0.4 \times 10^{26}$ dyne · cm.

The second event of the Ometepec doublet is slightly more complicated than the first one. This relative complexity is seen in the first pulse of WWSSN records, suggesting a double source for this event. Initially the P-wave data were modeled with a single source at a depth of 15 km and a source time function (7, 10, 17). The synthetic seismograms fit the overall waveform of the observed records at most stations, but not the near-nodal stations. A double-source model fits all the stations better. A comparison of the single and the double-source model for a station near the radiation pattern maximum, KEV, and a near-nodal station, ARE, clearly shows (Fig. 7) that the double source is better. The observed and synthetic P-waves recorded at 22 WWSSN and GDSN stations for the 1982 ^{2} Ometepec event (June 7, 1982, 10 h 59 min) are shown in Fig. 8. The first source is at a depth of 15 km with a source time function (3, 6, 8) and contributes 25% of the total seismic moment. The second source is located at 10 km depth with source time function (2, 6, 10), separated 6 s from the first source, and contributes 75% of the total seismic moment of the event. The orientation of the sources is similar. The separation between the two sources can be resolved to within 1 s, the time constants of the source time function are determined to ± 1 s, and the contribution of each source to the seismic moment is accurate to 10%. The depth of the first source is resolvable to within ± 3 km and the second source within ± 5 km. The orientation of the second source is controlled by the near-nodal stations (ZOBO, ARE, NNA, LPA) and its contribution to

TABLE IV

Results of body-wave modeling for the Ometepec doublet

Event	Source time		% M_0	Fault parameters				M_0 (10^{26} dyne·cm)
	Delay (s)	Function (s)		Depth (km)	Strike (φ)	Dip (δ)	Slip (λ)	
1982[1]	0	(2, 6, 8)	100%	20	293°	13°	78°	1.49
1982[2]	0	(3, 6, 8)	25%	15	296°	12°	90°	
	6	(2, 6, 10)	75%	10	285°	11°	66°	2.75

the total seismic moment by the waveforms at all stations. The seismic moment estimated at each station is given in Fig. 8 and the average moment from non-nodal stations within 30 and 90° is $M_0 = (2.8 \pm 0.6) \times 10^{26}$ dyne · cm.

Table IV summarizes the results from the body-wave modeling. Although the absolute depths determined by the modeling of body waves are shallower than those reported by the U.S.G.S. (40.5 and 33.8 km, respectively), the trend that the first event is deeper than the second is consistent with the U.S.G.S. results. Our depths are in good agreement with those determined by a local network, 25 and 8 km, respectively (Table VII).

3. Discussion

The results obtained by inversion of surface waves are in general consistent with those obtained by P-wave modeling. The seismic moments determined by the two methods are about the same for the second event of the doublet. However, for the first event the seismic moment determined by P-wave modeling is about half that obtained by surface-wave inversion (Tables III and IV).

The focal mechanisms indicate thrusting of the Cocos Plate under the North America Plate in a northeasterly direction with a small right lateral component (Figs. 6 and 8). These results are consistent with the relative plate motion (Minster and Jordan, 1978) and with local structures in the area, namely the right lateral displacement of the Ometepec Canyon (Shipley et al., 1980). The source time function of the events is simple, as other large events along the Middle America Trench (Chael and Stewart, 1982). Figure 9 shows the vertical component long-period WWSSN seismograms of P, PP and PPP waves from the Ometepec doublet and other large shallow ($M_s \geq 7$) subduction events that occurred along the Middle America Trench between 1965 and 1982 recorded at Eskdalemuir, Scotland (ESK). Notice the relatively simple waveforms of most events, and the smaller peak-to-peak amplitudes of the Ometepec doublet events.

3.1. Stress drops, fault dimensions and displacements

The stress drop of the events can be calculated from the relations for a dip-slip fault given by

$$\Delta\sigma = (8M_0)/(3\pi Lw^2) \qquad (1)$$

(e.g., Kanamori and Anderson, 1975). In the following calculations, we use the seismic moments determined by surface-wave inversion (Table III). The seismic moment for both events of the doublet is 5.6×10^{26} dyne · cm. The aftershock area from the first week of activity from P.D.E. is 80×40 km^2, consistent with the aftershock area determined by a local network (Nava, 1983), then we obtain $\Delta\sigma \approx 4$ bars from (1). This value is within the usual range of interplate earthquakes (Kanamori and Anderson, 1975), and is similar to those (1–10 bars) estimated for other large subduction events along the Middle America Trench (Table VII) using the same method.

To determine the stress drop of each of the events, it is necessary to know their fault areas. Unfortunately, the fault area of each event cannot be determined from the aftershock distribution (fig. 2b, S.K. Singh, 1983, personal communica-

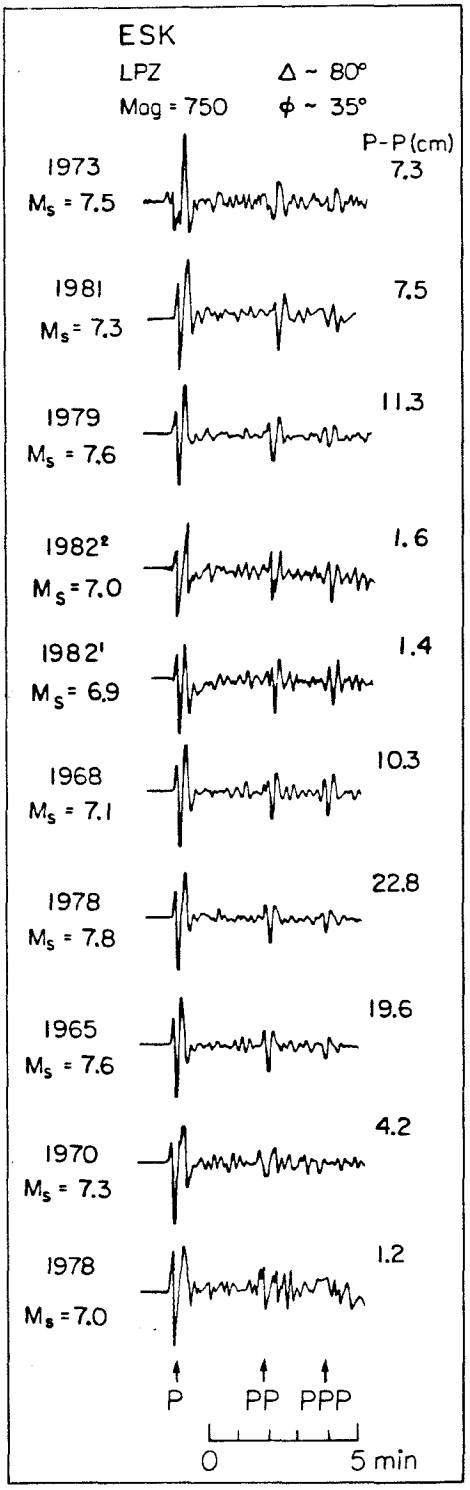

Fig. 9. Vertical long-period WWSSN seismograms of P, PP and PPP waves recorded at Eskdalemuir, Scotland (ESK), are shown for large shallow ($M_s > 7$) subduction events which occurred along the Middle America trench between 1965 and 1982. The events are ordered from west to east along the trench. Peak-to-peak amplitudes are given for each waveform (modified from Chael and Stewart, 1982). Note the relatively simple waveforms for most events and the small peak-to-peak amplitude of the Ometepec doublet.

tion). However, the fault dimensions of an earthquake can be inferred from the source time function (t_1, t_2, t_3) obtained from the P-wave modeling by assuming a particular fault rupture geometry: unilateral, bilateral, etc.. The fault length L can be estimated from the rupture time t_2 for a unilateral or a bilateral fault model by $t_2 \approx L/v_r$ or $t_2 \approx L/2v_r$, respectively, where v_r is the rupture velocity, here assumed to be 2.5 km s^{-1}. The unilateral fault model yields the minimum fault dimensions, whereas the maximum dimensions are given by the bilateral fault model. The source time function (2, 6, 8) of the 1982 [1] Ometepec event suggests fault lengths of 15 and 30 km for a unilateral and bilateral model, respectively. For the 1982 [2] Ometepec event, we use the single source time function (7, 10, 17) to represent the double source. Then the inferred fault lengths are 25 and 50 km for a unilateral and bilateral fault, respectively. If there is no overlap between the rupture zones of the two events, the length of the combined rupture zones is from 40 to 80 km. The fact that the seismic moment for the first event determined from body-wave data is almost half that from surface-wave data suggests that the body waves were generated from only part of the entire fault plane. Considering this, the fault length of 40–80 km estimated from body-wave data is in good agreement with the length of the aftershock area, 80 km.

The average displacement for each of the events can be estimated from the relation

$$M_0 = \mu DA \qquad (2)$$

where $\mu = 3 \times 10^{11}$ dyne cm^{-2}, D is the average displacement and A is the fault area. For $A = 3200$ km^2, D is estimated to be 0.58 m. The convergence

rate between the Cocos Plate and the North American Plate at the Ometepec region is 7 cm y^{-1} using the pole position given by Minster and Jordan (1978). The displacement, accumulated since the last large earthquake in the region in 1950, is 2.24 m. Thus the seismic slip averaged over the entire rupture zone is about 25% of the total slip accumulated during the previous 32 years. A similar ratio of the seismic slip to the total convergence between the Cocos and North America Plates has been suggested for the Petatlán area, further north along the Mexican subduction zone (Valdés et al., 1982). These values indicate moderate seismic coupling between these plates. However, south of the Tehuantepec Ridge large discrepancies between the convergence and seismic slip rate have been observed, indicating rather weak seismic coupling between the Cocos and the Caribbean Plates (McNally and Minster, 1981). Since 1902 there has been no truly great earthquake along the El Salvador and Nicaragua coasts (Fig. 11). Kanamori (1977) compared seismic slip with the rate of plate motion for various subduction zones, and concluded that the ratio of the seismic slip to the total slip, η, varies significantly from place to place; $\eta \approx 1$ for Chile, and possibly Alaska, $\eta \approx 1/4$ for the Kuriles Islands and northwestern Japan, and $\eta \approx 0$ for the Marianas. Sykes and Quittmeyer (1981) found that η ranges from 0.3 to 0.9 for various subduction zones, if it is computed with the time-predictable model of earthquake occurrence (Shimazaki and Nakata, 1980).

3.2. Doublets along the Middle America Trench

Along the Middle America Trench, seismic doublets similar to the 1982 Ometepec doublet are relatively frequent. Here we define a doublet by, a pair of large events with a magnitude difference of no more than 0.2 units, spatial separation < 100 km, and temporal separation < 3 years. The temporal separation is about 10% of the average recurrence time of large events along the Middle America Trench. Table V lists doublets according to this definition along the Middle America Trench. There are several regions in the world where doublets occur frequently; the Solomon Islands region (Lay and Kanamori, 1980) and south-west Japan (Ando, 1975) are among the typical examples.

Lay and Kanamori (1980) argue that the existence of relatively large isolated asperities (areas with increased strength) on the fault contact plane is responsible for the frequent occurrence of doublets in the Solomon Islands region. Other important features observed for the Solomon Islands region include, a relatively high plate convergence rate (11 cm y^{-1}), and short (30 y) recurrence times for large earthquakes. The subduction zone along the Middle America Trench exhibits many of these features, as discussed in the previ-

TABLE V
Seismic 'doublets' along the Middle America Trench

Region	Date	Time (h min.)	Location [a]			M_s	Time interval (h)
			Lat (°N)	Long (°W)	Depth		
6	May 11, 1962	1411	17.25	99.58	40[3]	7.0	
	May 19, 1962	1458	17.12	99.57	33[3]	7.2	192
7	June 7, 1982	0652	16.348	98.368	25[11]	6.9[6]	
	June 7, 1982	1059	16.399	98.538	8[11]	7.0[6]	4
8	August 4, 1928	1828	16.83	97.61[3]	S	7.4	
	October 9, 1928	0301	16.34	97.29[3]	S	7.6	1584
9	June 17, 1928	0319	16.33	96.70[3]	S	7.8[2]	
	January 15, 1931	0150	16.10	96.64[3]	S	7.8[2]	21852
18	April 24, 1916	0802	11	85	S	7.3	
	April 26, 1916	0221	10	85	S	7.3	42

[a] Superscripts indicate the reference numbers in Table VII.

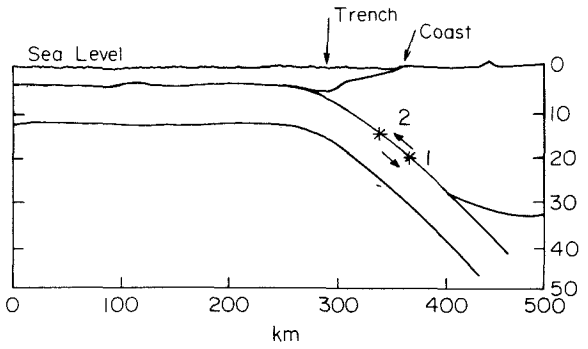

Fig. 10. Profile of the Middle America Trench near the Ometepec region after Couch and Woodcock (1981). Stars show the locations of the Ometepec doublets. Arrows indicate the relative motion between the plates. Note that the first event of the doublet is deeper than the second.

ous section. Also, Singh et al. (1982b) found that the number of large earthquakes ($M_s \geq 7$), which have occurred since 1904 along the Mexican subduction zone, is significantly larger than expected from the conventional magnitude-frequency relation. They suggest that the asperities which are responsible for these events are about the same size. This relatively uniform asperity size may be favorable for the occurrence of doublets.

Another important aspect of the doublet occurrence, is the triggering mechanism. Both of the Ometepec events have about the same seismic moment, 2.8×10^{26} dyne · cm. The hypocenter of the first event is deeper and its source time function is shorter by a factor of two, suggesting that the first event represents failure of a smaller and deeper asperity, and the failure of the deeper asperity triggered the shallower one (Fig. 10). The slip direction of the first event is perpendicular to the trench, forming a 13° angle with the convergence direction of the Cocos Plate at the Ometepec region, whereas the slip direction of the main source of the second event is parallel to it. A similar difference between the slip vectors of the doublet events is also observed for the Solomon Islands doublets. The difference, however, is small, since the subduction along this boundary is not as oblique as in the Middle America Trench. This difference may indicate that the first event of doublets, reflects more local stress heterogeneities on the fault plane, than the second one.

3.3. Seismic moment versus recurrence time

In the present study, we consider a simple asperity model in which the fault contact plane is held by discrete asperities (places with increased strength), each surrounded by weak regions. For simplicity, we assume that the slip on the asperities are completely seismic, and the slip in the weak zone is aseismic during the interseismic period. When an asperity breaks, causing a seismic event, some coseismic slip accompanies in the surrounding region. Hence, the rupture zone that is responsible for seismic radiation is larger than the asperity. A simple mechanical model corresponding to this situation has been considered by Madariaga (1977) and Rudnicki and Kanamori (1981). We let u, A and D be the amount of slip on the asperity, the area of the entire rupture zone and the slip averaged over the rupture zone, respectively. The seismic moment, M_0, measured by surface waves is then given by (2). Since the gross stress drop in large earthquakes is constant (e.g., Kanamori and Anderson, 1975)

$$M_0 \approx D^3 \tag{3}$$

In this model, the slip on the asperity is equal to the slip accumulated by plate motion

$$u = VT \tag{4}$$

where V is the plate convergence rate and T is the repeat time. The ratio of the seismic slip, averaged over the entire rupture zone to the total plate motion during the interseismic period is

$$\eta = D/VT = D/u \tag{5}$$

We showed earlier that $\eta = 0.25$ in the Ometepec region. Combining (3), (4) and (5) we have

$$T = \frac{u}{V} = \frac{D}{\eta V} \approx \frac{1}{\eta V} M_0^{1/3} \tag{6}$$

Hence, we expect that along a given subduction zone where the convergence rate, V, and η are approximately constant

$$\log T \approx \tfrac{1}{3} \log M_0 \tag{7}$$

Although the size and rupture length of historical events along the Middle America Trench are somewhat uncertain, we attempt to test this relation with the data presently available. Figure 11 is

TABLE VI

Observed recurrence period T, of large, shallow, interplate earthquakes along Middle America

Region		Year of earthquake (M_s)						T (y)
1	Jalisco	1837 (7.7)	1875 (7.4)	1900 (7.9) [1900 (7.4)] [d]	1932 (8.2) [1934 (7.0)] [d]			31.7 ± 6.5
2	Colima	[1806 (7.5)] [d]	[1818 (7.7) [d]	1911 (7.7)	1932 (7.8)	1941 (7.7)	1973 (7.5)	21.3 ± 10.5
3	Michoacan						1981 (7.3)	–
4	Petatlan				1908 (7.5)	1943 (7.5)	1979 (7.6)	35.5 ± 0.7
5	Guerrero	1887 (7.2) [1889 (7.2)] [d]	1899 (7.9)	1909 (7.4)				–
6	Acapulco	[1820 (7.6)] [d]	1845 (7.9)	1907 (8.0)		1957 (7.5) [1962 (7.0)] [d] [1962 (7.2)] [d]		56.0 ± 8.5 [c]
7	Ometepec		1890 (7.2)		1937 (7.5)	1950 (7.3)	1982 (6.9) [1982 (7.0)] [d]	30.6 ± 17.0
8	West Oaxaca	1854 (7.7)	1894 (7.4)		1928 (7.6) [1928 (7.4)] [d]	1968 (7.4)		38.0 ± 3.5
9	Central Oaxaca		1870 (7.4) [1872 (7.9)] [d]		1928 (7.8) [1931 (7.8)] [d]		1978 (7.8)	53.0 ± 4.2

10	East Oaxaca		1897 (7.4)		1928 (7.5)	1965 (7.6)		34.5 ± 3.6
11	Tehuantepec							
12	Chiapas			1902 (8.2)	1944 (7.0)	1970 (7.3)		34.0 ± 11.3
13	W. Guatemala				1919 (7.0)	1950 (7.1)		31.5
14	E. Guatemala		1862 [a]	1902 (7.9)		1942 (7.9)		40.0 ± 0.0
15	El Salvador		1859 [a]	1901 (7.9)	1926 (7.1)			33.5 ± 12.0
16	W. Nicaragua		1850 [b]	1901 (7.6)	1921 (7.3)			35.5 ± 21.9
17	E. Nicaragua	1881 [a] 1885 [a]	1898 (7.5)			1956 (7.3)		25.0 ± 28.9
18	Costa Rice		1851 [b]	1916 (7.3) [1916 (7.3)] [d]	1939 (7.3)	1950 (7.7)	1978 (7.0)	20.7 ± 8.7
19	Cocos				1924 (7.0)	1952 (7.2)	1983 (7.2)	29.5 ± 2.1
20	West Panama			1904 (7.6)	1941 (7.5)			37.0
21	East Panama			1934 (7.7)		[1962 (7.0)] [d] 1962 (7.4)		28.0

[a] Large earthquake from Carr and Stoiber (1977).
[b] Great earthquake from Carr and Stoiber (1977).
[c] T for events with $M_s \geq 7.4$.
[d] Events not used to estimate the recurrence time T.

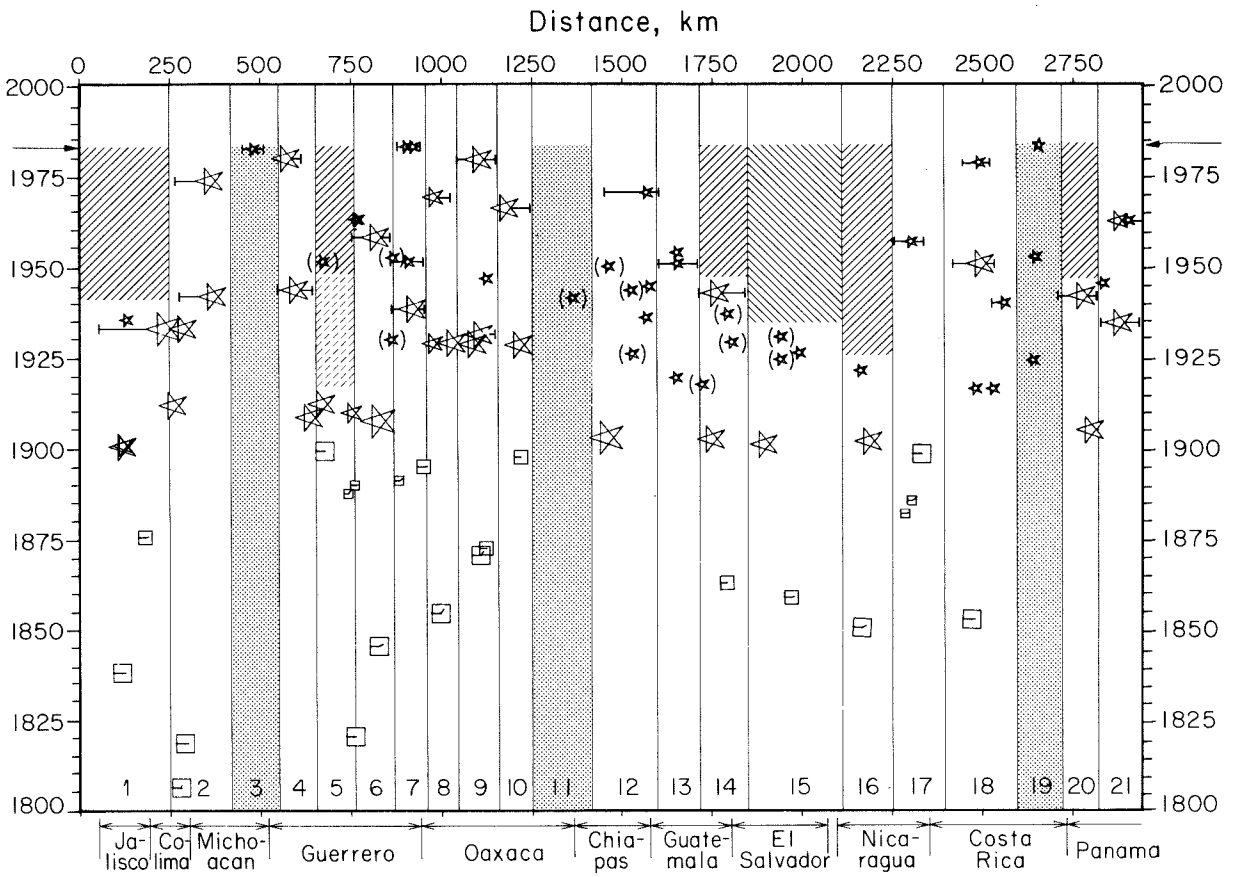

Fig. 11. Time-distance plot along the Middle American Trench. Symbols are the same as in Fig. 1. Events listed by Miyamura (1976) as $M = 7$ are in parentheses. Names at the bottom refer to Mexican coastal states and Central American countries. Numbers at the bottom indicate regions determined from aftershock area distributions. Dotted regions correspond to the Orozco fracture zone (3) and the Tehuantepec (11) and Cocos (19) Ridges where seismicity has been lower in number and magnitude than other regions, at least during this century. Hatched sections indicate seismic gaps: Jalisco (1), Guerrero (5), Guatemala (14), El Salvador (15), Nicaragua (16) and West Panama (20).

a time-distance plot of large shallow events ($M > 7$) along the Middle America Trench. Event locations are taken from a recompilation made by Singh et al. (1981) for the Mexico region and from Stoiber and Carr (1973) and McNally and Minster (1981) for Central America. Events listed by Miyamura (1976) as $M = 7$ are in parentheses in Fig. 11 and are not listed in Table VI, since they are likely to be < 7 (see Singh et al., 1981, table 3).

The entire region is subdivided into 21 regions as shown in Fig. 11. This division is made mainly on the basis of the distribution of aftershock areas of recent events (Kelleher et al., 1973; Reyes et al., 1979; Singh et al., 1980a; Guendel and McNally, 1982; Valdés et al., 1982; Havskov et al., 1983). Three dotted regions corresponding to the Orozco fracture zone (3), the Tehuantepec (11) and Cocos (19) Ridges are defined on the basis of the absence of seismicity. In these regions, no earthquake larger than 7.3 has occurred during this century. The Tehuantepec region is considered aseismic or seismic with anomalously large recurrence intervals (McCann et al., 1978; Singh et al., 1980a). Regions where no large, shallow interplate earthquake has occurred for more than 30 years are hatched in Fig. 11. These regions are considered

seismic gaps with high potential, since the average recurrence interval for this type of earthquake is 33 ± 8 years (McNally and Minster, 1981). The Jalisco (1), Guerrero (5), Guatemala (14), El Salvador (15), Nicaragua (16) and West Panama (20) gaps fall in this category, and special attention should be directed to these areas.

Table VI shows the year and magnitude of the events which occurred in each region. The average recurrence interval, T, is calculated from $\frac{1}{n}\sum_{i=1}^{n} t_i$, where n is the number of intervals and t_i is the time interval in years between consecutive events. Events not used to estimate T are in parentheses. Only those events which occurred after 1820 are used to estimate the average recurrence intervals for each region. If the interval between two consecutive events is less than 3 years, the events are grouped together as a single sequence. In the Jalisco region (1), the events which occurred in 1900 (7.4) and 1934 (7.0) are probably aftershocks of the 1900 (7.9) and 1932 (8.2) earthquakes, respectively.

TABLE VII

Source parameters of large shallow intraplate Middle America earthquakes

Date	Location			M_s	M_W	$\Delta\sigma$ (bars)	M_{ob} [a] (10^{27} dyne·cm)	M_{os} [b]
	Lat (°N)	Long (°W)	Depth					
April 15, 1907	16.7	99.2 [c]	S	8.0 [d]	7.8			5.9 [n]
June 17, 1928	16.33	96.7 [e]	S	7.8 [d]	7.7			3.9 [o]
January 15, 1931	16.10	96.64 [e]	S	7.8 [d]	7.6			3.4 [o]
June 3, 1932	19.84	103.99 [e]	S	8.2 [d]	7.9			9.1 [o]
June 18, 1932	19.5	103.5 [g]	S	7.8 [d]	7.8			7.3 [o]
December 23, 1937	17.1	98.07 [e]	S	7.5	7.4			1.5 [p]
August 6, 1942	13.9	90.9 [e]	S	7.9 [d]	7.6			4.1 [o]
December 14, 1950	17.22	98.12 [e]	S	7.3 [g]	7.1			0.6 [p]
July 28, 1957	17.11	99.10 [e]	S	7.5 [i]	7.6			3.3 [n]
August 23, 1965	16.024	95.928	24.7 [f]	7.6 [i]	7.5	6	1.9	1.7 [q]
April 2, 1968	16.394	98.056	21 [f]	7.1 [g]	7.3	4	0.8	1.0 [q]
April 29, 1970	14.52	92.60	33	7.3 [g]	7.4	1	0.5	1.2 [q]
January 30, 1973	18.39	103.21	32 [j]	7.5 [g]	7.6	7		3.0 [q]
November 29, 1978	15.767	96.800	18 [f]	7.8 [g]	7.6	8	1.9	3.2 [q]
March 14, 1979	17.454	101.455	13.6 [k]	7.6 [g]	7.6	10	1.0	2.7 [q]
October 25, 1981	17.75	102.25	20 [l]	7.3 [g]	7.3	50		1.4 [r]
June 7, 1982	16.348	98.368	25 [m]	6.9 [h]	6.9	4	0.15	0.27 [s]
June 7, 1982	16.399	98.538	8 [m]	7.0 [h]	6.9	4	0.27	0.25 [s]

[a] M_{ob}, seismic moment from body waves.
[b] M_{os}, seismic moment from surface waves.
[c] Figueroa, 1970.
[d] Geller and Kanamori, 1977.
[e] Kelleher et al., 1973.
[f] Tajima and McNally, 1983.
[g] NOAA.
[h] PDE.
[i] Abe and Kanamori, 1980.
[j] Reyes et al., 1979.
[k] Gettrust et al., 1981.
[l] Havskov et al., 1983.
[m] Emilio Nava, personal communication.
[n] Singh et al., 1982a.
[o] Wang et al., 1982.
[p] S.K. Singh, written communication.
[q] Chael and Stewart, 1982.
[r] Lefevre and McNally, 1982.
[s] This study.

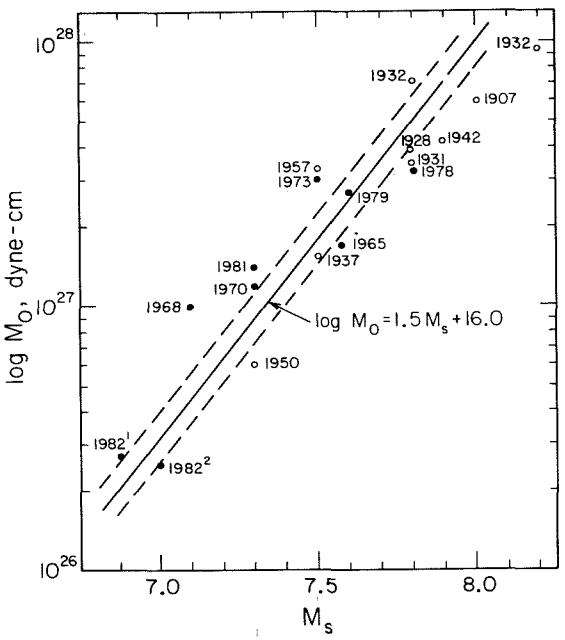

Fig. 12. Relation between M_s (20s surface-wave magnitude) and M_0 (seismic moment) for events that have occurred along the Middle America subduction zone. The dashed lines correspond to $\log M_0 = 1.5\ M_s + (16.0 \pm 0.1)$ Open circles are estimates from one station. Solid circles are estimates from several stations.

In the Acapulco region (6), the 1962 doublet is considered to be part of the activity associated with the 1957 (7.5) Acapulco earthquake. Only the time of occurrence of the first event, of those listed as doublets in Table V, is used to estimate the average recurrence interval in the Ometepec (7), West Oaxaca (8), Central Oaxaca (9) and Costa Rica (18) regions. In the East Panama region (21), the 1962 (7.0) earthquake is probably a foreshock of the 1962 (7.4) event. The Guerrero region (5) has not experienced a major earthquake in the last 74 years; since most of the historic events are clustered in a 22 year-period, no reliable recurrence period can be determined.

Table VII is a compilation of focal parameters for some large, shallow interplate earthquakes which occurred along the Middle America Trench. The moment-magnitude relation for these events is shown in Fig. 12. The relation

$$\log M_0 = 1.5\ M_s + 16.0 \qquad (8)$$

shown by a heavy line fits the data well. The average seismic moment, $\overline{M}_0$, for each region is obtained from events which occurred during this century from $\frac{1}{n}\Sigma_{i=1}^{n} M_{0_i}$, where n is the number of events and M_{0_i} is the seismic moment for each event. If the seismic moment of the event is known, as listed in Table VII, it is used for calculating the average. If not, it is estimated from the surface-wave magnitude using (8). If consecutive events occur < 3 years apart, they are treated as a single event and their moments are added and considered a single value. Table VIII gives the average seismic moment for regions along Mexico. The data are insufficient for Central America regions. To calculate the corrected recurrence time period,

TABLE VIII

Average seismic moment $\overline{M}_0$, for regions along the Mexican subduction zone

Region	$\overline{M}_0$ (10^{27} dyne·cm)	V (cm y^{-1})	T (y)	T_c (y)
1. Jalisco	8.75 ± 0.92	5.14	31.7 ± 6.5	23.2 ± 6.5
2. Colima	4.35 ± 1.98	5.27	21.3 ± 10.5	16.0 ± 10.5
3. Michoacan				
4. Petatlan	2.24 ± 0.54	6.22	35.5 ± 0.7	31.5 ± 0.7
5. Guerrero				
6. Acapulco	5.08 ± 1.16	6.71	56.0 ± 8.5	53.7 ± 8.5
7. Ometepec	0.88 ± 0.56	7.00	30.6 ± 17.0	30.6 ± 17.0
8. W. Oaxaca	2.39 ± 1.95	7.07	38.0 ± 3.5	38.4 ± 3.5
9. C. Oaxaca	5.25 ± 2.89	7.30	53.0 ± 4.2	55.3 ± 4.2
10. E. Oaxaca	1.74 ± 0.05	7.50	34.5 ± 3.6	36.9 ± 3.6
11. Tehuantepec				

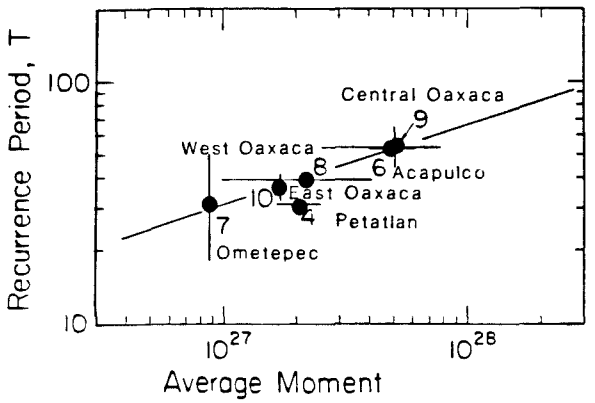

Fig. 13. Plot of average seismic moment $\bar{M}_0$ (dyne·cm), versus recurrence period T (years), for each region along the Mexican subduction zone (Table VIII). The lines have a slope of 1/3, suggesting that the relation $\log T \approx 1/3 \log M_0$ holds for the Guerrero–Oaxaca region along the Mexican subduction zone. Numbers correspond to regions listed in Tables VI and VIII.

T_c, to a uniform velocity of 7 cm y^{-1} at each region; we multiply the recurrence period, T, at the region by $V/7$, where V is the corresponding plate velocity. This correction, however, is negligible for the Guerrero–Oaxaca (4–10) regions. The plate velocities given for each region are computed for the Cocos plate pole (Minster and Jordan, 1978). The relation between $\bar{M}_0$ and T_c is shown in Fig. 13 for regions along the Mexican subduction zone. The heavy line has a slope of 1/3. Despite the relatively large error bars associated with each region, the data for the Guerrero–Oaxaca regions (4–10) follow the relation given by (7), supporting the simple asperity model.

The events in the Jalisco and Colima regions do not follow the trend for the Guerrero–Oaxaca region. The plate geometry is more complex northwest of the Michoacan gap, than in the Guerrero–Oaxaca region, and factors other than the asperity size may have to be considered in estimating the repeat time.

4. Conclusion

Table III summarizes the source parameters of the 1982 Ometepec earthquakes, determined by inversion of long-period surface-wave data. Table V lists the source parameters obtained by waveform modeling of long-period P waves. Adding the seismic moments for the two events obtained by surface-wave inversion and using the fault size inferred from the aftershock area, we estimate the stress drop and the amount of slip to be about 3.5 bars and 0.58 m. The amount of coseismic displacement is approximately a quarter of the total slip accumulated during the previous 32 years since the last large earthquake in the region, suggesting that seismic slip takes up 25% of the plate motion.

For large earthquakes in the Guerrero–Oaxaca region, we found a relation $\log T \approx 1/3 \log M_0$ where T is the average repeat time and M_0 is the average moment of the characteristic events of a sequence which occurred at approximately the same place. This relation suggests that the scale length of asperities controls the repeat time, if other factors such as the plate convergence rate and η are approximately the same.

A review of seismicity along the Middle America Trench shows that some regions, along Jalisco, Guerrero, Guatemala, El Salvador, Nicaragua and West Panama have not had a large earthquake for more than 30 years, and are considered seismic gaps with high seismic potential.

Acknowledgments

The authors thank Emilio Nava and Shri K. Singh for providing us with aftershock information, prior to publication, Thorne Lay for helpful discussion and encouragement throughout this study and Jeff Given for computer programs. We thank Holly Eissler, Jeff Given and Thorne Lay for helpful comments on the manuscript. Seismograms were kindly sent by many of the WWSSN stations. The IDA data used in this study were made available to us by courtesy of the IDA project team and the Institute of Geophysics and Planetary Physics, University of California, San Diego. This work was partially supported by U.S. Geological Survey contract 14-08-0001-21223. Contribution 3955, Division of Geological and Planetary Sciences, California Institute of Technology, Pasadena, CA 91125, U.S.A.

References

Abe, K. and Kanamori, H., 1980. Magnitude of great shallow earthquakes from 1953–1977. Tectonophysics, 62: 191–203.

Ando, M., 1975. Source mechanisms and tectonic significance of historical earthquakes along the Nankaido trough, Japan. Tectonophysics, 27: 119–140.

Aubouin, J., Stephan, J.F., Renard, V., Roump, J. and Lousdale, P., 1981. Subduction of the Cocos plate in the Mid America Trench, Nature, 294: 147–150.

Carr, M.J. and Stoiber, R.E., 1977. Geologic setting of some destructive earthquakes in Central America. Geol. Soc. Am. Bull., 88: 151–156.

Chael, E.P. and Stewart, G.S., 1982. Recent large earthquakes along the Middle American Trench and their implications for the subduction process. J. Geophys. Res., 87: 329–338.

Couch, R. and Woodcock, S., 1981. Gravity and structure of the continental margins of southwestern Mexico and northwestern Guatemala. J. Geophys. Res., 86: 1829–1840.

Dean, B.W. and Drake, C.L., 1978. Focal mechanism solutions and tectonics of the Middle America arc. J. Geol., 86: 111–128.

Demaint, A., 1978. Caracteristicas del Eje Neovolcanico Transmexicano y sus problemas de interpretacion. Rev. Inst. Geol. U.N.A.M., 2: 172–187.

Dziewonski, A.M., Chou, T.-A. and Woodhouse, J.H., 1981. Determination of earthquake source parameters from wave-form data studies of global and regional seismicity. J. Geophys. Res., 86: 2825–2852.

Eissler, H. and Kanamori, H., 1982. A large normal-fault earthquake at the junction of the Tonga trench and the Lousville ridge. Phys. Earth Planet. Inter., 29: 161–172.

Espindola, J.M., Singh, S.K., Yamamoto, J. and Havskov, J., 1981. Seismic moments of large Mexican subduction earthquakes since 1907. EOS, 62: 948.

Figueroa, J., 1970. Catálogo de sismos ocurridos en la Republic Mexicana. Report 272, Instituto de Ingenieria, U.N.A.M., Mexico, 88pp.

Fisher, R.L., 1961. Middle America trench: topography and structure. Geol. Soc. Am. Bull., 72: 703–720.

Geller, R.J., 1976. Scaling relations for earthquake source parameters and magnitudes. Bull. Seismol. Soc. Am., 66: 1501–1523.

Geller, R.J. and Kanamori, H., 1977. Magnitude of great shallow earthquakes from 1904–1952. Bull. Seismol. Soc. Am., 67: 587–598.

Gettrust, J.F., Hsu, V., Helsley, C.E., Herrero, E. and Jordan, T., 1981. Patterns of local seismicity preceding the Petatlan earthquake of March 14, 1979. Bull. Seismol. Soc. Am., 71: 761–769.

Guendel, F. and McNally, K.C., 1982. The foreshock–mainshock–aftershock sequence of the 1978 ($M_s = 7.0$) Samara, Costa Rica earthquake: A unique data set. Abstracts with Programs Seismol. Soc. Am., 53: 81.

Havskov, J., Singh, S.K., Nava, E., Dominguez, T. and Rodriguez, M., 1983. Playa Azul, Michoacan, Mexico, earthquakes of 25 October, 1981 ($M_s = 7.3$). Bull. Seismol. Soc. Am., 73: 449–458.

Kanamori, H., 1977. Seismic and aseismic slip along subduction zones and their tectonic implications. Maurice Ewing series 4, Earthquake Prediction Research, 4: 163–174.

Kanamori, H., 1983. Use of long-period surface waves for fast evaluation of tsunami potential of large earthquakes. Summaries of Technical Reports XVI Open-file report, 83–525.

Kanamori, H. and Anderson, D.L., 1975. Theoretical basis of some empirical relations in seismology. Bull. Seismol. Soc. Am., 65: 1073–1093.

Kanamori, H. and Stewart, G.S., 1976. Mode of strain release along the Gibbs fracture zone, Mid-Atlantic Ridge. Phys. Earth Plant. Inter., 11: 312–332.

Kanamori, H. and Given, J., 1981. Use of long-period surface waves for rapid determination of earthquake-source parameters. Phys. Earth Planet. Inter., 27: 8–31.

Kanamori, H. and Given, J., 1982. Use of long-period surface waves for rapid determination of earthquake-source parameters. 2. Preliminary determination of source mechanisms of large earthquakes ($M_s \geq 6.5$) in 1980. Phys. Earth Planet. Inter., 30: 260–268.

Kelleher, J., Sykes, L. and Oliver, J., 1973. Possible criteria for predicting earthquake locations and their application to major plate boundaries on the Pacific and the Caribbean. J. Geophys. Res., 78: 2547–2585.

Langston, C.A. and Helmberger, D.V., 1975. A procedure for modelling shallow dislocation sources. Geophys. J.R. Astron. Soc., 42: 117–130.

Lay, T. and Kanamori, H., 1980. Earthquake doublets in the Solomon Islands. Phys. Earth Planet. Inter., 21 283–304.

Lay, T. and Kanamori, H., 1981. An asperity model of large earthquakes sequences. Maurice Ewing Series 4, Earthquake Prediction Research, 1: 3–71.

Lay, T., Given, J. and Kanamori, H., 1982. Long period mechanism of the 8 November, 1980, Eureka, CA earthquake. Bull. Seismol. Soc. Am., 72: 439–456.

Lefevre, V. and McNally, K., 1982. Stress distribution in the Mexican subduction zone. EOS, 63: 1039–1040.

Madariaga, R., 1977. Implications of stress-drop models of earthquakes for the inversion of stress drop from seismic observations. Pure Appl. Geophys., 115: 301–316.

Mamerickx, J., Smith, S.M., Taylor, I.L. and Chase, T.E., 1975. Topography of the South Pacific. Carte Bathymetrique, Scripps Institution of Oceanography, La Jolla, CA.

McCann, W.R., Nishenko, S.P., Sykes, L. and Krause, J., 1979. Seismic gaps and plate tectonics: seismic potential for major boundaries. Pageoph., 117: 1082–1147.

McNally, K. and Minster, J.B., 1981. Non-uniform seismic slip rates along the Middle America trench. J. Geophys. Res., 86: 4949–4959.

Minster, J.B. and Jordan, T.H., 1978. Present day plate motions. J. Geophys. Res., 83: 5331–5354.

Miyamura, S., 1976. Provisional magnitudes of Middle American earthquakes not listed in the magnitude catalogue of Gutemberg–Richter. Bull. Int. Inst. Seismol. Earthquake Eng., 14: 41–46.

Molnar, P. and Sykes, L., 1969. Tectonics of the Caribbean and Middle America regions from focal mechanisms and seismicity. Geol. Soc. Am. Bull., 80: 1639–1684.

Mooser, F., 1972. The Mexican volcanic belt: structure and tectonics. Geofiz. Int., 17: 55–70.

Nakanishi, I. and Kanamori, H., 1982. Effects of lateral heterogeneity and source process time on the linear moment tensor inversion of long-period Rayleigh waves. Bull. Seismol. Soc. Am., 72: 2063–2080.

Nava, E.A., 1983. Estudio de los temblores de Ometepec del 7 de junio de 1982 y sus réplicas. Tesis Profesional, Facultad de Ingeniería, UNAM.

Ohtake, M., Matumoto, T. and Latham, G.V., 1977. Seismic gap near Oaxaca, southern Mexico as probable precursor to a large earthquake. Pageoph., 115: 375–385.

Plafker, G., 1976. Tectonic aspects of the Guatemala earthquake of 4 February, 1976. Science, 193: 1201–1208.

Reyes, A., Brune, J.N. and Lomnitz, C., 1979. Source mechanism and aftershock study of the Colima, Mexico earthquake of January 30, 1973. Bull. Seismol. Soc. Am., 69: 1819–1840.

Rudnicki, J.W. and Kanamori, H., 1981. Effects of fault interaction on moment, stress drop and strain energy release. J. Geophys. Res., 86: 1785–1793.

Shipley, T., McMillen, K.J., Watkins, J.S., Moore, J.C., Sandoval-Ochoa, J.H. and Worzel, J.L., 1980. Continental margin and lower slope structures of the Middle America trench near Acapulco (Mexico). Mar. Geol., 35: 65–82.

Shimazaki, K. and Nakata, T., 1980. Time-predictable recurrence model for large earthquakes. Geophys. Res. Lett., 7: 279–282.

Singh, S.K., Yamamoto, J., Havskov, J., Gusmán, M., Novelo, D. and Castro, R., 1980a. Seismic gap of Michoacan, Mexico. Geophys. Res. Lett., 7: 69–71.

Singh, S.K., Havskov, J., McNally, K., Ponce, L., Hearn, T. and Vassiliou, M., 1980b. The Oaxaca, Mexico earthquake of 29 November, 1978: A preliminary report on aftershocks. Science, 207: 1211–1213.

Singh, S.K., Astiz, L. and Havskov, J., 1981. Seismic gaps and recurrence periods of large earthquakes along the Mexican subduction zone: A reexamination. Bull. Seismol. Soc. Am., 71: 827–843.

Singh, S.K., Epiñdola, J.M., Yamamoto, J. and Havskov, J., 1982a. Seismic potential of Acapulco–San Marcos region along the Mexican subduction zone. Geophys. Res. Lett., 9: 633–636.

Singh, S.K., Rodriguez, M. and Esteva, L., 1982b. Statistics of small earthquakes and frequence of occurrence of large earthquakes along the Mexican subduction zone. EOS, 63: 1040 pp.

Stewart, G.S., Chael, E.P. and McNally, K., 1981. The November 29, 1979, Oaxaca Mexico earthquakes. A large simple event. J. Geophys. Res., 86: 5053–5060.

Stoiber, R.E. and Carr, M.J., 1973. Quaternary volcanic and tectonic segmentation of Central America. Bull. Volcanol., 37: 304–325.

Sykes, L.R. and Quittmeyer, R.C., 1981. Repeat times of great earthquakes along simple plate boundaries. Maurice Ewing series 4 Earthquake Prediction Research, 4: 217–247.

Tajima, F. and McNally, K.C., 1983. Seismic rupture patterns in Oaxaca, Mexico. J. Geophys. Res., 88: 4263–4276.

Valdés, C., Meyer, R.P., Zúniga, R., Havskov, J. and Singh, S.K., 1982. Analysis of the Petatlán aftershocks: number, energy release and asperities. J. Geophys. Res., 87: 8519–8527.

Yamamoto, J., 1978. Rupture processes of some complex earthquakes in southern Mexico. Ph.D. Thesis, Saint Louis University, MO, 203 pp.

Wang, S., McNally, K. and Geller, R.J., 1982. Seismic strain release along the Middle America trench, Mexico. Geophys. Res. Lett., 9: 182–185.